Use of JMP® Software to Optimize Low Temperature Cofired Ceramics Laser Cavity Formation through Design of Experiments

Melvin T. Alexander, Westinghouse, Baltimore, MD
Brian Hogan, Independent Project Analysis, Inc., Reston VA
Carl T. Brooks, Westinghouse, Baltimore, MD

Abstract

Design of Experiments (DOE) is a proven statistical quality tool that identifies processing parameters, interactions between processing parameters, and optimum parameter settings in manufacturing processes. When applied to process development of new electronic packaging technologies, e.g., Low Temperature Cofired Ceramics (LTCC) Laser Cavity Formation processes, the results of DOE can characterize the output, optimize the through-put, and achieve consistent quality in a minimal number of experimental runs.

This paper will show how JMP® software was applied to optimize the LTCC Laser Cavity formation process through various statistical viewpoints (e.g., exploratory, nonparametric, parametric, and Bayesian). JMP's data visualization features gave fresh clues to manufacturing process engineers about those "active" input factors that influenced the key characteristics (cavity location and ceramic tape peel-off). The statistical approaches distinguish between the "active" and "inactive" factors that may not be evident using only the singular methods. Significant factors consistently identified by all strategies tell the data analyst and manufacturing engineers which factors to control and compare with confirmation runs so that process optimization is maintained.

Introduction

Low Temperature Cofired Ceramic (LTCC) is a glass ceramic composite which provides an extremely versatile approach to high performance, highly integrated electronic packaging. LTCC substrates in multilayer format allow designers to integrate both RF and digital interconnections in a single, self-contained hermetic unit. Monolithic LTCC structures incorporating buried components allow increased design flexibility by providing a mechanism for establishing both microstrip and stripline within thesame medium. The ability to integrate digital, analog, RF, buried microwave, and buried components in this manner reduces assembly complexity and improves overall component and system reliability by reducing part and interface counts.

Cavity formation of the LTCC is a key aspect of the integrated packages. Requirements for the cavity formation process include: 1) flexibility to form cavities on multiple types of material 2) high throughput to meet production quantities 3) capability to form a wide range of cavity sizes, 4) acceptable quality with respect to size, location, and tape edge condition, and 5) compatibility with the common carrier used for material handling throughout the process.

Common methods for forming cavities in LTCC include numerically-controlled punching, router bits, a CO_2 laser, and a die punch.

During the laser cavity formation development process, parameter settings on the equipment were frequently being modified in order to form acceptable cavities with various designs. While equipment settings were adequate for a specific cavity size and material, these same settings may result in the LTCC sticking to the tooling plate on the next package design. As a result, Design of Experiments was applied to optimize the laser cavity formation process.

Goals and Objectives

The goal of this case study is to optimize the laser cavity formation process for LTCC material systems by maximizing through-put while maintaining consistant quality. The objective was to identify the key processing parameters which impacted the quality of the cavitiy, and determine the levels which optimized the resilts for the laser-cavity formation process.

Plan

JMP® software helped to meet the objectives by applying statistical Design of Experiments to identify the key processing parameters which impacted the quality characteristics. The **Screening Fit** option was selected over the **MANOVA** because it was better suited for the optimizing the factor-level setting rather than determining statistical significance of model effects. A team consisting of LTCC manufacturing engineers and operations division statistician determined the quality characteristics, the cavity file layout, the processing factors to investigate, the levels to vary, the experimental array layout, and the measurement methodology. Quality was measured by the cavity dimensions in the x-(horizontal) and y-(vertical) directions and the variability of that dimension. Peel off measured the amount of resistance of ceramic tape that stuck to the tooling nestplate when the material was removed. If peel off is poor, the tape stuck to the nestplate and increased opportunities for microcracks along cavity edges to appear. Good peel off meant that tape was easily removed from the tooling nestplate with good quality cavity edges. In order to optimize the process on multiple material systems, the experiment layouts with different levels will be run and analyzed separately on two different tape systems, Tape 1 and Tape 2.

In order to evaluate a wide range of cavity styles, the cavity file generated for the experiment included a sampling of the cavity dimensions already designed. Three cavities were formed for each run, two for each with style including Cavity (1) small square cavity (75 mils x 75 mils), Cavity (2) medium square cavity (200 mils x 200 mils), and Cavity(3) large square cavity (approximately 500 mils x 500 mils).

During the laser process development, the most common factors changed to improve the quality of various cavities formed in different materials included the table velocity, table acceleration, and the laser power. Along with significantly impacting the throughput of the process, we believed that thesefactors would have strong interactions between each other. The current settings for the Tape 1 were velocity of 1.5, acceleration of 1.5, and laser power of 7%. The current settings for the Tape 2 were velocity of 2.5, acceleration of 2.5, and laser power of 20%

After selecting the factors, the levels to vary for the experiment were determined. In order to optimize throughput of the process, higher settings for the velocity and acceleration were selected to evaluate. Table 1 summarizes the factors and levels for the experiment with each material system.

Table 1. Laser Cavity Factors and Levels

	Level	Level	Level
Tape 1	1	2	3
Velocity	1.5	2.0	2.5
Acceleration	1.5	2.0	2.5
Power	7%	13%	20%
Tape 2			
Velocity	2.5	3.0	3.5
Acceleration	2.5	2.0	1.5
Power	20%	25%	30%

After selecting the factors and levels, an experimental array was selected based upon experience, we expected correlations between the power and velocity and acceleration. That is, as the velocity increased, more power would be required to form cavities in the material. The experimental array selected was a 9-run experiment based on previous Taguchi studies.

The cavity file layout was step 'n' repeated once for each run of the experiment for 2 repetitions. The peel-off of the tape was qualitatively measured for each tape piece on a scale of 1 to 3, with 1 being good peel-off (no resistance) and 3 being poor peel-off (resistance resulting in rejectable material). The dimensions of three cavities were measured with an x-y motion table and quantitatively analyzed. The three cavities selected for evaluation were the high aspect ratio cavity, the large square cavity, and the small square cavity. Ten measurements were taken for each repetition of each run. In order to account for any bowing of the cavity edge as a result of the increased velocity, measurements were taken at corner as well as at edges of the selected cavities.

Results

The data results were analyzed using JMP® software to produce Regression/Analysis of Variance (ANOVA) models, Interaction Profile plots, and Box-Meyer Bayes plots for the response variables (Peel off, X, and Y dimensions). Regression formed statistical models through combinations of single, second-order and interacting factor effects to characterize the responses. Table 2 summarized the ANOVA results. For Peel off, more than 92 percent of the variation was explained by significant effects of Velocity, Acceleration, Power, Tape, Velocity*Acceleration and Power* Tape intereactions and Acceleration*Accelration as a second-order term.

Table 2. Summary of Fit and ANOVA Effects Test for Peel off

Peel off Quality

Summary of Fit

RSquare	0.921228
RSquare Adj	0.899659
Root Mean Square Error	0.251438
Mean of Response	2.027778
Observations (or Sum Wgts)	108

Source	Nparm	DF	Sum of Squares	F Ratio	Prob>F
Velocity	1	1	0.2595	4.1043	0.0459
Acceleration	1	1	0.2555	4.0416	0.0476
Velocity*Acceleration	1	1	0.5206	8.2344	0.0052
Power	1	1	0.6820	10.7876	0.0015
Velocity*Power	1	1	0.8790	13.9044	0.0003
Acceleration*Power	1	1	0.1773	2.8051	0.0977
Tape	1	1	0.2568	4.0615	0.0471
Velocity*Tape	1	1	0.1576	2.4926	0.1181
Acceleration*Tape	1	1	0.0096	0.1511	0.6985
Power*Tape	1	1	0.4845	7.6628	0.0069
Cavity	2	2	0.0000	0.0000	1.0000
Velocity*Cavity	2	2	0.0000	0.0000	1.0000
Acceleration*Cavity	2	2	0.0000	0.0000	1.0000
Power*Cavity	2	2	0.0000	0.0000	1.0000
Tape*Cavity	2	2	0.0000	0.0000	1.0000
Velocity*Velocity	1	1	0.0229	0.3627	0.5486
Acceleration*Acceleration	1	1	0.5389	8.5242	0.0045
Power*Power	1	1	0.1029	1.6272	0.2056

For the X dimension, about 64.2 percent of the variation was explained in RSquare (R^2) by Cavity, and Tape*Cavity (see Table 3).

Table 3. Summary of Fit and ANOVA Effects Test for X Dimension

x dim

Summary of Fit

RSquare	0.642108
RSquare Adj	0.544111
Root Mean Square Error	1.589574
Mean of Response	-0.80361
Observations (or Sum Wgts)	108

Source	Nparm	DF	Sum of Squares	F Ratio	Prob>F
Velocity	1	1	4.5019	1.8274	0.1801
Acceleration	1	1	2.4015	0.9748	0.3263
Velocity*Acceleration	1	1	0.0002	0.0001	0.9927
Power	1	1	4.6219	1.8761	0.1744
Velocity*Power	1	1	5.2030	2.1120	0.1499
Acceleration*Power	1	1	5.1621	2.0954	0.1515
Tape	1	1	4.9522	2.0102	0.1599
Velocity*Tape	1	1	4.5146	1.8326	0.1795
Acceleration*Tape	1	1	1.9054	0.7734	0.3817
Power*Tape	1	1	4.0510	1.6444	0.2033
Cavity	2	2	24.4961	4.9717	0.0091
Velocity*Cavity	2	2	5.0842	1.2105	0.3032
Acceleration*Cavity	2	2	3.8898	0.8098	0.4484
Power*Cavity	2	2	11.1680	2.2865	0.1100
Tape*Cavity	2	2	33.1738	7.1388	0.0014
Velocity*Velocity	1	1	3.5858	1.4474	0.2323
Acceleration*Acceleration	1	1	3.8376	1.5578	0.2155
Power*Power	1	1	0.0723	0.0294	0.8644

We expected more significant factors would stand out in the analysis. For the Y dimension (Table 4), about 82.3 percent of the variation was explained by the Tape*Cavity interaction.

Table 4. Summary of Fit and ANOVA Effects Test for Y Dimension

y dim

Summary of Fit

RSquare	0.821639
RSquare Adj	0.772802
Root Mean Square Error	0.572815
Mean of Response	0.690083
Observations (or Sum Wgts)	108

Source	Nparm	DF	Sum of Squares	F Ratio	Prob>F
Velocity	1	1	0.0511212	0.1557	0.6941
Acceleration	1	1	0.0000510	0.0002	0.9901
Velocity*Acceleration	1	1	0.6904008	2.1034	0.1507
Power	1	1	0.0170992	0.0521	0.8200
Velocity*Power	1	1	0.0013359	0.0041	0.9493
Acceleration*Power	1	1	0.2245612	0.6842	0.4105
Tape	1	1	0.0499113	0.1521	0.6976
Velocity*Tape	1	1	0.1120026	0.3412	0.5607
Acceleration*Tape	1	1	0.0197440	0.0602	0.8069
Power*Tape	1	1	0.0044864	0.0137	0.9072
Cavity	2	2	0.6143167	0.9356	0.3963
Velocity*Cavity	2	2	0.7061444	1.0757	0.3457
Acceleration*Cavity	2	2	0.2288028	0.3452	0.7081
Power*Cavity	2	2	0.0845643	0.1288	0.8793
Tape*Cavity	2	2	3.2888741	4.9766	0.0091
Velocity*Velocity	1	1	0.2572417	0.7837	0.3785
Acceleration*Acceleration	1	1	0.0122506	0.0373	0.8473
Power*Power	1	1	0.2408306	0.7337	0.3941

We chose to keep the non significant effects in order to enhance the predictive capability of the models. Significant two-factor interactions with non-significant single factors can occur whenever the factor level means do not disclose definite effects or when there is confounding present among other factors. Confounding (or aliasing) makes it difficult to tell which factors affect Peel off, and the X and Y dimensions because the significant factors mask or resemble the effects of other single and interacting factors. Traditional approaches to deal with this problem are to run additional experiments that will remove the confounding, or carefully examine the confounding structure exhibited by the factors. Both approaches were complicated to comprehend, costly to implement, and sometimes overlook important factors. Other ways to circumvent these difficulties without doing more costly runs were thorough examination of Interaction Profile plots (Figures 1, 2, and 3), Normal Probability Plots (Figures 4, 5, and 6) and Box-Meyer Bayes plots (Figures 7, 8, and 9).

The significant Tape*Cavity interaction in Figure 1 does not show very much for Peel off.

Figure 1. Interactions Plot of Peel Off

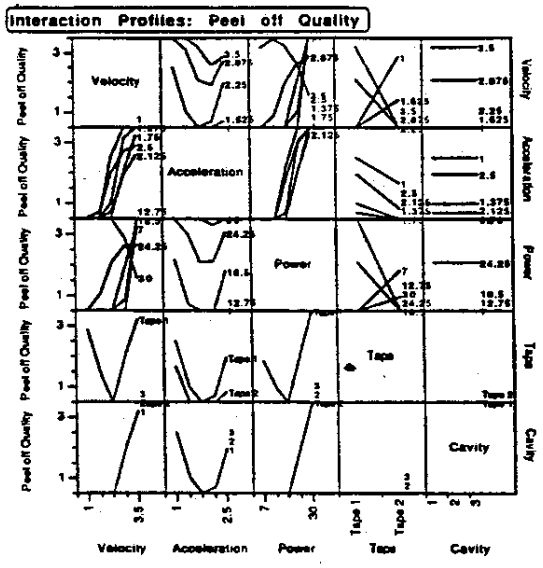

For the X- dimension (Figure 2), Cavity differences were wider for Tape 1 than for Tape 2. Midsized cavities seem to closer to target than the other cavities for both the X and Y dimensions.

Figure 2. Interactions Plot of the X Dimension

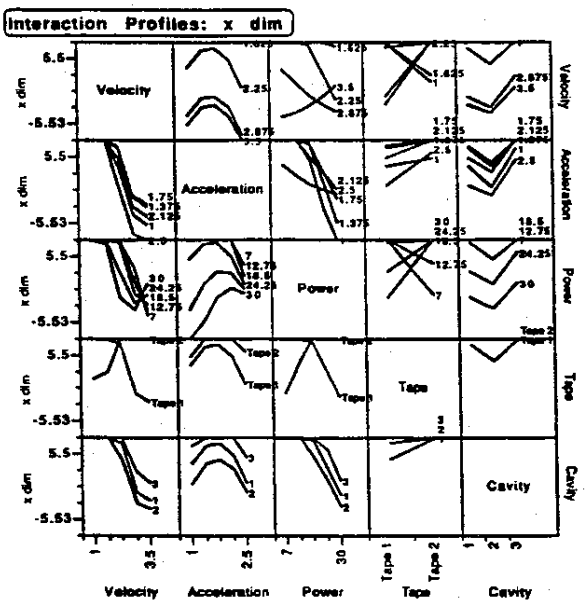

The interaction profile plot for the Y-dimension (Figure 3) shows that high power settings have smaller Tape effect differences than low power levels. In other words, Tape 1 has smaller effect differences with increased power levels than Tape 2.

Figure 3. Interactions Plot of the Y Dimension

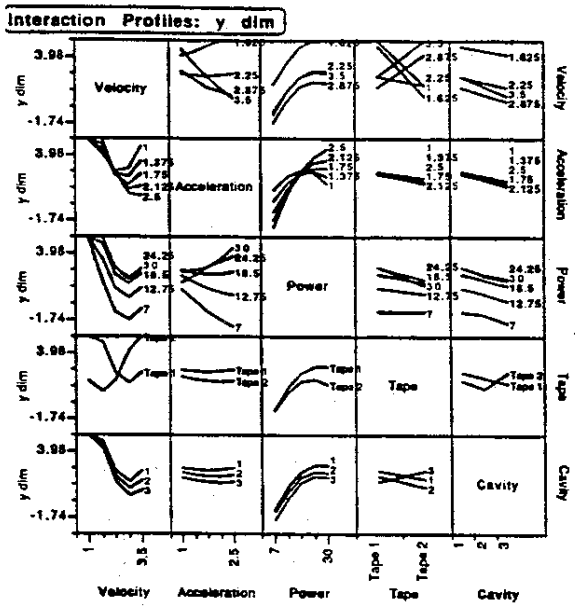

Figures 4-6 display the Normal probability plots for the three responses. The active factors were identified the more they strayed away from the Length's PSE (nonparametric) and RMSE (parametric) normality lines.

Figure 4. Normal Probability Plot of Peel Off

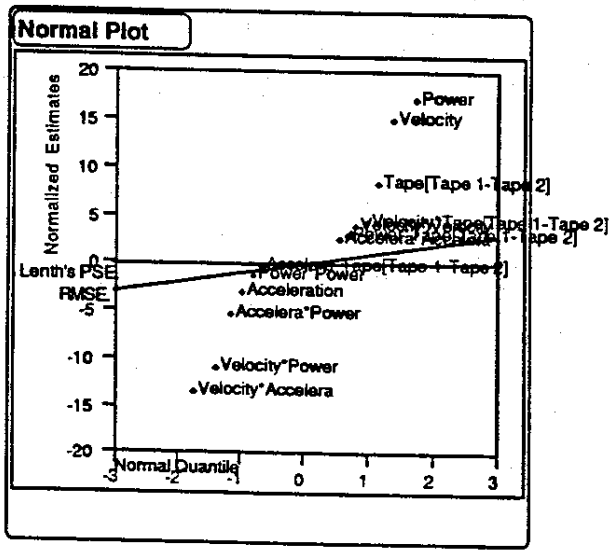

Figure 5. Normal Probability Plot of the X Dimension

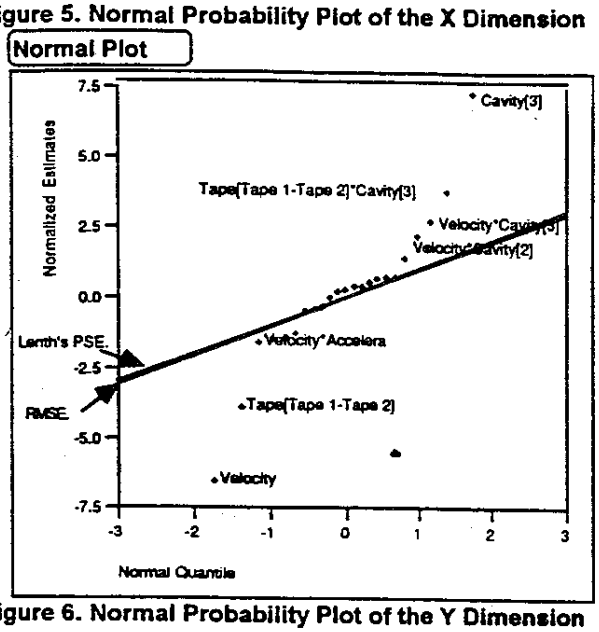

Figure 6. Normal Probability Plot of the Y Dimension

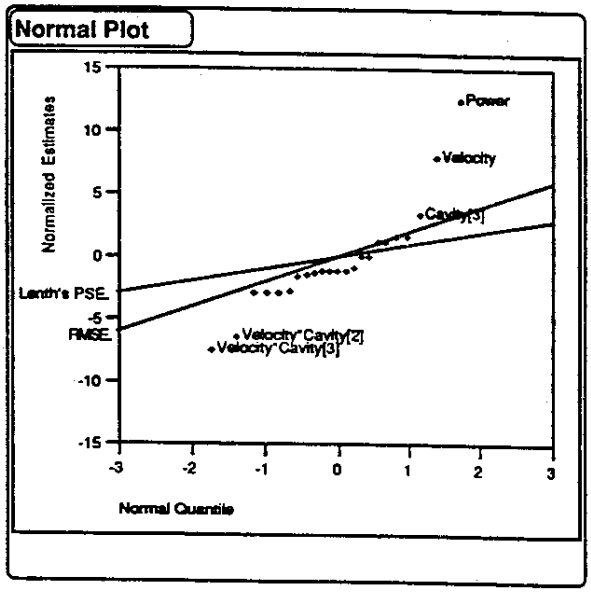

Box-Meyer Bayes plots (Figures 7- 9) showed the "active" (or important) factors affecting Peel off, X-, and Y-dimensions. The Box-Meyer Bayesian approach took the regression model developed earlier and assigned prior probabilities of significance to each of the single and interacting factors. These factors had prior probabilities set to 20 percent (i.e., each **Prior** = 0.20). Next, posterior probabilities (**Posterior**) were computed for these factors, conditional upon the assumption that some factors inflated the random error (or noise, **Std Err Est**=1) variance by a multiple of ten (i.e., **K Contam**=10). The active factors had posterior probabilities 60 percent or greater (i.e., **Posterior** ≥ 0.60). Inactive factors had posterior probabilities under 50 percent. For Peel off, the active factors were Velocity, Acceleration, Power, and Tape for

main effects, Velocity*Acceleration,Velocity*Power, Acceleration*Power, Velocity*Tape interactions, and Velocity*Velocity as the second order term.

Figure 7. Box-Meyer Bayes Plot of Peel Off

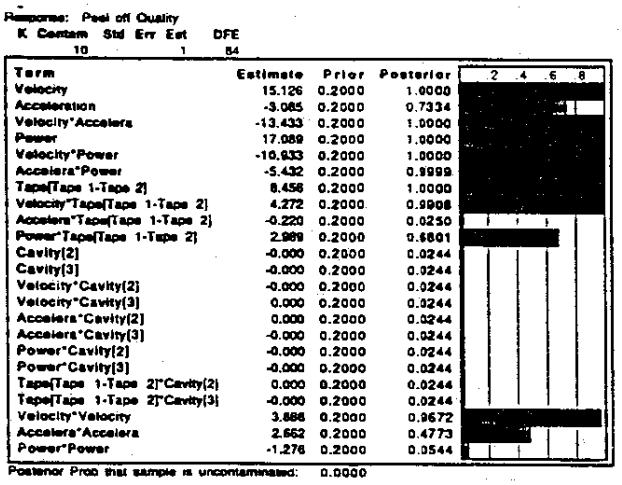

Response: Peel off Quality
K Contam Std Err Est DFE
10 1 84

Term	Estimate	Prior	Posterior
Velocity	15.126	0.2000	1.0000
Acceleration	-3.085	0.2000	0.7334
Velocity*Accelera	-13.433	0.2000	1.0000
Power	17.089	0.2000	1.0000
Velocity*Power	-10.933	0.2000	1.0000
Accelera*Power	-5.432	0.2000	0.9999
Tape[Tape 1-Tape 2]	8.456	0.2000	1.0000
Velocity*Tape[Tape 1-Tape 2]	4.272	0.2000	0.9908
Accelera*Tape[Tape 1-Tape 2]	-0.220	0.2000	0.0250
Power*Tape[Tape 1-Tape 2]	2.989	0.2000	0.6801
Cavity[2]	-0.000	0.2000	0.0244
Cavity[3]	-0.000	0.2000	0.0244
Velocity*Cavity[2]	-0.000	0.2000	0.0244
Velocity*Cavity[3]	0.000	0.2000	0.0244
Accelera*Cavity[2]	0.000	0.2000	0.0244
Accelera*Cavity[3]	-0.000	0.2000	0.0244
Power*Cavity[2]	-0.000	0.2000	0.0244
Power*Cavity[3]	-0.000	0.2000	0.0244
Tape[Tape 1-Tape 2]*Cavity[2]	0.000	0.2000	0.0244
Tape[Tape 1-Tape 2]*Cavity[3]	-0.000	0.2000	0.0244
Velocity*Velocity	3.886	0.2000	0.9672
Accelera*Accelera	2.662	0.2000	0.4773
Power*Power	-1.276	0.2000	0.0544

Posterior Prob that sample is uncontaminated: 0.0000

The active factors for the X-dimension were the single factors Velocity, Tape, and Cavity size {large versus all other factor levels}. Power*Tape and Tape*Cavity{midsize versus all other levels} were the significant interactions.

Figure 8. Box-Meyer Bayes Plot of the X Dimension

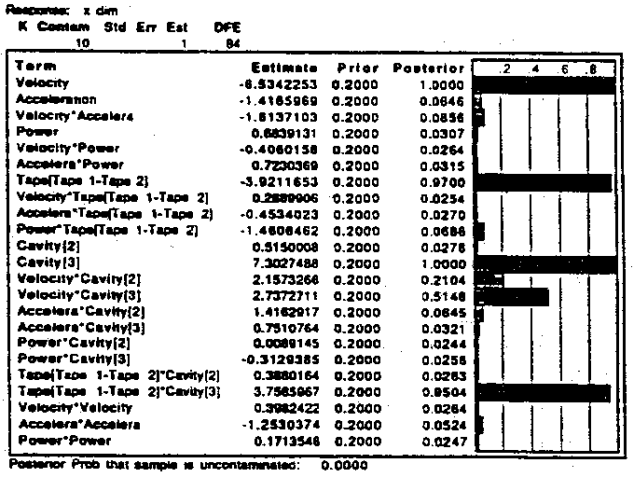

Response: x dim
K Contam Std Err Est DFE
10 1 84

Term	Estimate	Prior	Posterior
Velocity	-6.5342253	0.2000	1.0000
Acceleration	-1.4165969	0.2000	0.0646
Velocity*Accelera	-1.8137103	0.2000	0.0856
Power	0.6839131	0.2000	0.0307
Velocity*Power	-0.4060158	0.2000	0.0264
Accelera*Power	0.7230369	0.2000	0.0315
Tape[Tape 1-Tape 2]	-3.9211653	0.2000	0.9700
Velocity*Tape[Tape 1-Tape 2]	0.2889906	0.2000	0.0254
Accelera*Tape[Tape 1-Tape 2]	-0.4534023	0.2000	0.0270
Power*Tape[Tape 1-Tape 2]	-1.4606462	0.2000	0.0686
Cavity[2]	0.5150008	0.2000	0.0276
Cavity[3]	7.3027488	0.2000	1.0000
Velocity*Cavity[2]	2.1573266	0.2000	0.2104
Velocity*Cavity[3]	2.7372711	0.2000	0.5148
Accelera*Cavity[2]	1.4162917	0.2000	0.0645
Accelera*Cavity[3]	0.7510764	0.2000	0.0321
Power*Cavity[2]	0.0089145	0.2000	0.0244
Power*Cavity[3]	-0.3129385	0.2000	0.0258
Tape[Tape 1-Tape 2]*Cavity[2]	0.3880164	0.2000	0.0263
Tape[Tape 1-Tape 2]*Cavity[3]	3.7565967	0.2000	0.9504
Velocity*Velocity	0.3982422	0.2000	0.0264
Accelera*Accelera	-1.2530374	0.2000	0.0524
Power*Power	0.1713546	0.2000	0.0247

Posterior Prob that sample is uncontaminated: 0.0000

For the Y-dimension, the active single factors were Velocity, Power, and Cavity for {large versus all other levels}. The active interacting factors were Velocity*Acceleration, Power*Tape, Velocity *Cavity{midsized versus all other levels} and {large versus all others}.

Figure 9. Box-Meyer Bayes Plot of the Y Dimension

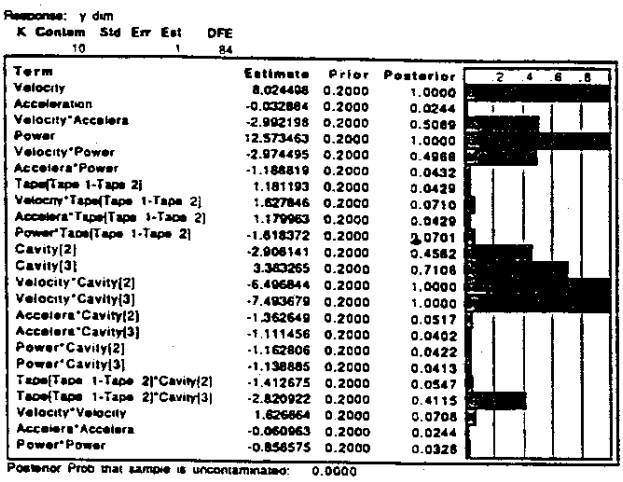

Response: y dim
K Contam Std Err Est DFE
10 1 84

Term	Estimate	Prior	Posterior
Velocity	8.024498	0.2000	1.0000
Acceleration	-0.032884	0.2000	0.0244
Velocity*Accelera	-2.992198	0.2000	0.5089
Power	12.573463	0.2000	1.0000
Velocity*Power	-2.974495	0.2000	0.4988
Accelera*Power	-1.188819	0.2000	0.0432
Tape[Tape 1-Tape 2]	1.181193	0.2000	0.0429
Velocity*Tape[Tape 1-Tape 2]	1.627846	0.2000	0.0710
Accelera*Tape[Tape 1-Tape 2]	1.179963	0.2000	0.0429
Power*Tape[Tape 1-Tape 2]	-1.618372	0.2000	0.0701
Cavity[2]	-2.906141	0.2000	0.4582
Cavity[3]	3.363265	0.2000	0.7106
Velocity*Cavity[2]	-6.496844	0.2000	1.0000
Velocity*Cavity[3]	-7.493679	0.2000	1.0000
Accelera*Cavity[2]	-1.362649	0.2000	0.0517
Accelera*Cavity[3]	-1.111456	0.2000	0.0402
Power*Cavity[2]	-1.162806	0.2000	0.0422
Power*Cavity[3]	-1.138885	0.2000	0.0413
Tape[Tape 1-Tape 2]*Cavity[2]	-1.412675	0.2000	0.0547
Tape[Tape 1-Tape 2]*Cavity[3]	-2.820922	0.2000	0.4115
Velocity*Velocity	1.626864	0.2000	0.0708
Accelera*Accelera	-0.060963	0.2000	0.0244
Power*Power	-0.856575	0.2000	0.0328

Posterior Prob that sample is uncontaminated: 0.0000

If the same single and interacting factors were significant according to all analytical methods, then they could be considered as active in the laser cavity process. However, conflicting findings between the regression, ANOVA, and Box-Meyer approaches resulted. Box and Meyer showed that their Bayesian method was superior to other methods because it is completely general, considers other possible explanation of the data, e.g., large posterior probabilities, handles missing data, and revealed clues about the impact of hidden, overlooked interactions missed by the conventional methods. Also the method adequately treats factor settings that deviate from those originally planned. Two factors, unknown at the time the study was conducted, may account for the differences between the X- and Y- dimensions. One, engineers had to tune the amplifiers and servomotors of the equipment that overshot movement of the X-Y table. The table overshot by seven-tenths mils and returned to its original reference-target position. The equipment manufacturer came in end tuned the amplifiers to minimize the amount the X-Y table overshot. This could help explain the impact of Power , Velocity, and interactions in overshooting the X-Y table. Second, there were inherent differences between the X- and Y-axes. The Y-axis moved the table only. The X-axis moved both the table and Y-axis because it carried more weight than the Y-axis alone by its design. Therefore, it was difficult to tell if the differences between the X- and Y dimensions were due to the weight carried by the X-axis or due to the amplifier tuning. In other words there was confounding present.

OPTIMIZATION SUMMARY

The optimum settings seem to be very tape and cavity dependent. One tape system (Tape 2) was more robust than the other on the X and Y dimensions for various power, and velocity equipment settings, without the consideration of Peel off. Table functioning, equipment tuning amplifiers and servomotors, and inherent differences in the X- and Y-axes may have acted as confounding factors that accounted for the conflicting identification of active single and interacting factors. Table 5 showed the optimal equipment settings for velocity, acceleration, and power for both tapes and the different sized cavities. These settings were chosen based upon examination of the interaction plots, Prediction Profile plots (Figures 10-a through 10-f), and Correlations/Scatterplot Matrix (Figure 11) for the three responses. The Prediction profile plot uses Desirability functions of Derringer and Suich (1980). Desirability functions were appealing because, according to Goik et al. (1994), they combined engineering knowledge gained about the LTCC process and statistical knowledge formed by the fitted model of the **Parameter Estimates** table (Table 6) and predicted variation. Each response model was converted into individual desirability measures. Desirability functions helped choose the factor levels that maximizes the geometric mean of individual desirability functions of each response, i.e., $D=(d_{po}*d_x*d_y)^{1/3}$ where d_{po} is the desirability function for Peel off, d_x and d_y are the desirability functions for the X and Y dimensions, respectively. The high desirability values were "lower-the better" value (1-best) for Peel off and zero (0-nominal, ± 2.5 mils) as the "target-the-best" values for the X- and Y dimensions. Overall Desirability values ≥ 0.6000 represent acceptable quality above the best commercial practices. Even though interaction effects can render Desirability functions as misleading, see SAS Institute Inc. (1994), Chang and Shivpuri (1994) showed that they were acceptable "compromise optimal solutions" for multiple responses. These equipment settings served as recommendations to be compared with confirmation experiments to check validity and predictability.

TABLE 5. Optimal Settings of Power, Velocity and Acceleration for Tapes and Cavity Sizes

	CAVITY SIZE		
Tape 1	1	2	3
Velocity	2.85	2.85	3.27
Accelearation	1.80	1.61	2.13
Power	14.2	12.8	23.5
Desirability	0.8562	0.9645	0.7752
Tape 2	1	2	3
Velocity	1.55	1.55	1.55
Accelearation	1.19	1.38	1.05
Power	12.0	18.5	8.4
Desirability	0.8694	0.8250	0.8922

In conclusion, more follow up experiments need to be performed. The results provide a next step and strategy for better understanding the laser cavity process so that further optimization and improvement can be obtained.

REFERENCES

Box, G.E.P. and Meyer, R.D., (1993), "Finding the Active Factors in Fractionated Screening Experiments," *Journal of Quality Technology*, 25, 94-105.

Chakrabborty, A.K. and Borah, G.K. (1989), "An Application of the Concept of Desirability Functions in Evaluating Erection Quality," *Quality Engineering*, 1, 443-452.

Chang, S.I. and Shivpuri, R. (1994)
"A Multiple-Objective Decision-Making Approach for Assessing Simultaneous Improvement in Die Life and Casting Quality in a Die Casting Progress," *Quality Engineering*, 7, 371-384.

Derringer, G. and Suich, R., (1980), "Simultaneous Optimization of Several Response Variables," *Journal of Quality Technology*, 12, 214-219.

Goik, P., Liddy, J.W., and Taam, W., (1994), "Use of Desirability Functions to Determine Operating Windows for New Product Designs," *Quality Engineering*, 7, 267-276.

SAS Institute Inc., (1994), *JMP® Statistics and Graphics Guide*, Cary, NC: SAS Institute Inc., 178.

Figure 10-e. Prediction Profile Plot of Responses Across Velocity, Acceleration, Power, Tape 1, Cavity 1

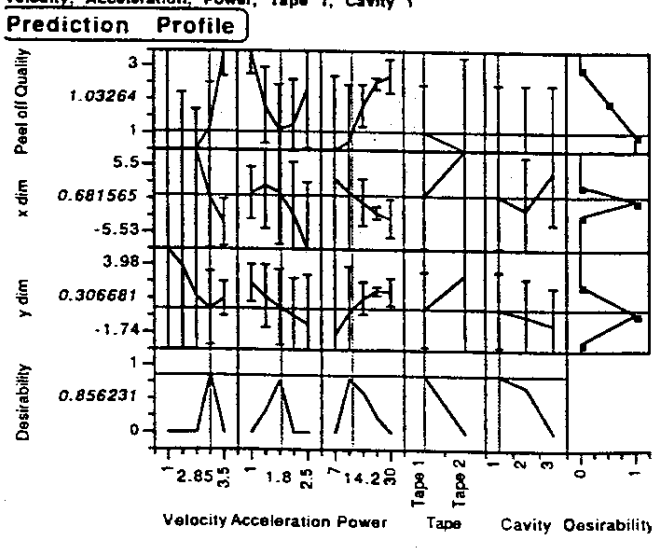

Figure 10-b. Prediction Profile Plot of Responses Across Velocity, Acceleration, Power, Tape 1, Cavity 2

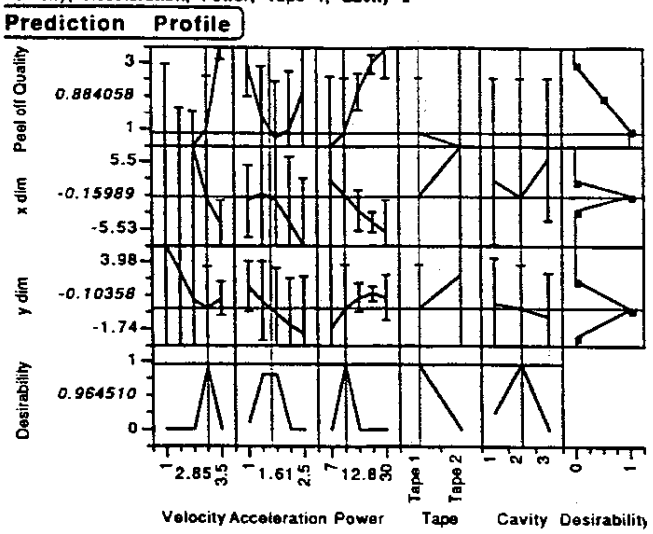

Figure 10-c. Prediction Profile Plot of Responses Across Velocity, Acceleration, Power, Tape 1, Cavity 3

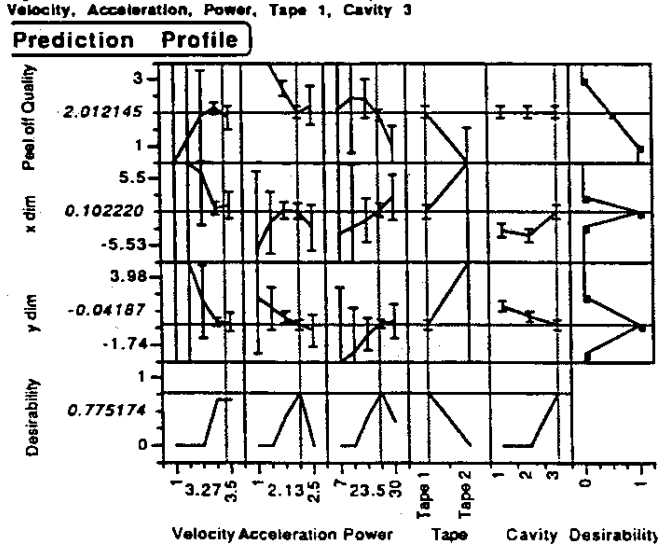

Figure 10-d. Prediction Profile Plot of Responses Across Velocity, Acceleration, Power, Tape 2, Cavity 1

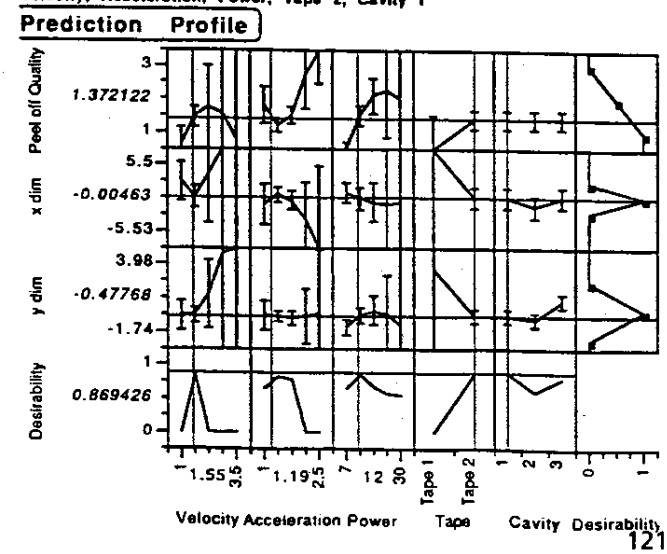

Figure 10-e. Prediction Profile Plot of Responses Across Velocity, Acceleration, Power, Tape 2, Cavity 2

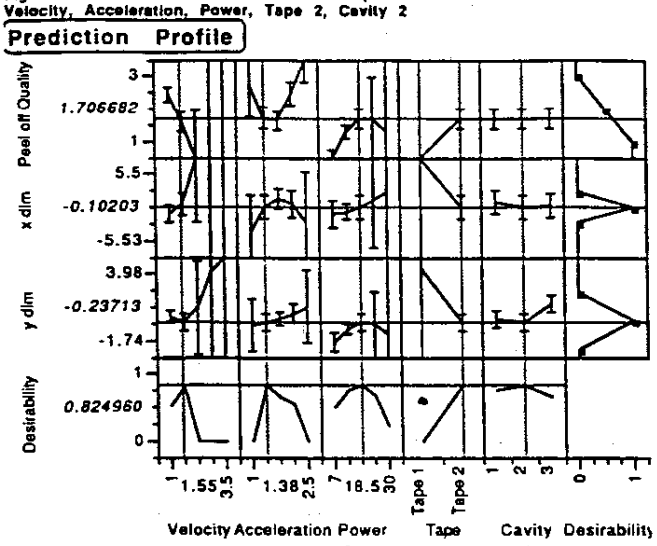

Figure 10-f. Prediction Profile Plot of Responses Across Velocity, Acceleration, Power, Tape 2, Cavity 3

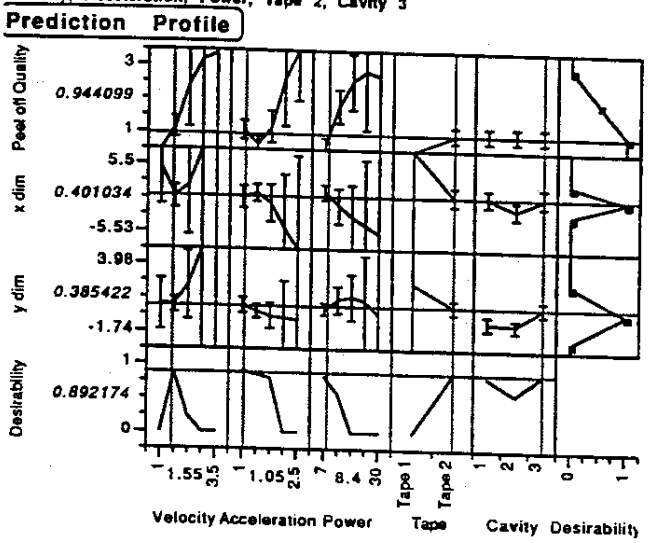

Table 6. Parameter Estimates for the Fitted Model of Responses

Parameter Estimates

	Peel off Quality	x dim	y dim
Intercept	-24.0778	93.3371	5.3791
Velocity	13.1206	-54.6514	-5.8236
Acceleration	-4.2615	13.0846	-0.6602
Velocity*Accelera	-2.0166	0.0402	-2.3224
Power	1.3772	-3.5851	0.2181
Velocity*Power	-0.3582	0.8665	-0.0139
Accelera*Power	-0.1800	0.8631	0.1600
Tape[Tape 1-Tape 2]	-13.4156	58.8159	5.9147
Velocity*Tape[Tape 1-Tape 2]	3.3546	-17.9552	-2.8281
Accelera*Tape[Tape 1-Tape 2]	0.0941	-1.3286	0.1352
Power*Tape[Tape 1-Tape 2]	0.3229	-0.9337	0.0311
Cavity[2]	-0.0000	-6.6233	0.3510
Cavity[3]	-0.0000	9.1924	0.9347
Velocity*Cavity[2]	0.0000	0.9908	-0.2317
Velocity*Cavity[3]	0.0000	-1.3842	-0.2533
Accelera*Cavity[2]	-0.0000	1.0617	-0.1933
Accelera*Cavity[3]	0.0000	-0.1408	-0.0725
Power*Cavity[2]	0.0000	0.0704	-0.0135
Power*Cavity[3]	-0.0000	-0.1856	0.0113
Tape[Tape 1-Tape 2]*Cavity[2]	-0.0000	-1.4292	0.0832
Tape[Tape 1-Tape 2]*Cavity[3]	-0.0000	3.4807	-0.9535
Velocity*Velocity	-0.6730	8.3921	2.2540
Accelera*Accelera	3.2625	-8.7063	0.4919
Power*Power	-0.0086	0.0055	-0.0100

Figure 11. Correlations and Scatterplot Matrix for the Responses

Correlations

Variable	Peel off Quality	x dim	y dim
Peel off Quality	1.0000	-0.2056	0.5964
x dim	-0.2056	1.0000	-0.1328
y dim	0.5964	-0.1328	1.0000

Scatterplot Matrix